

## **General Disclaimer**

### **One or more of the Following Statements may affect this Document**

- This document has been reproduced from the best copy furnished by the organizational source. It is being released in the interest of making available as much information as possible.
- This document may contain data, which exceeds the sheet parameters. It was furnished in this condition by the organizational source and is the best copy available.
- This document may contain tone-on-tone or color graphs, charts and/or pictures, which have been reproduced in black and white.
- This document is paginated as submitted by the original source.
- Portions of this document are not fully legible due to the historical nature of some of the material. However, it is the best reproduction available from the original submission.

NASA-17573

Unclas  
08605

(NASA-CR-170720) STUDY OF CERTAIN TETHER  
SAFETY ISSUES AND THE USE OF TETHERS FOR  
PAYLOAD ORBITAL TRANSFER. CONTINUATION OF  
INVESTIGATION OF ELECTRODYNAMIC  
STABILIZATION AND (Smithsonian Astrophysical G3/15

STUDY OF  
CERTAIN TETHER SAFETY ISSUES

AND

THE USE OF TETHERS FOR

ORBITAL TRANSFER

CONTINUATION OF  
INVESTIGATION OF ELECTRODYNAMIC STABILIZATION AND  
CONTROL OF LONG ORBITING TETHERS

Contract NAS8-33691

Semi-Annual Report

For the period 1 March 1981 thru 31 August 1981

Principal Investigator

Dr. Giuseppe Colombo

August 1981

Smithsonian Institution  
Astrophysical Observatory  
Cambridge, Massachusetts 02138

The Smithsonian Astrophysical Observatory  
and the Harvard College Observatory  
are members of the  
Center for Astrophysics

ORIGINAL PAGE IS  
OF POOR QUALITY.



**STUDY OF  
CERTAIN TETHER SAFETY ISSUES  
AND  
THE USE OF TETHERS FOR  
PAYLOAD ORBITAL TRANSFER**

**CONTINUATION OF  
INVESTIGATION OF ELECTRODYNAMIC STABILIZATION AND  
CONTROL OF LONG ORBITING TETHERS**

**Contract NAS8-33691**

**Semi-Annual Report  
For the period 1 March 1981 thru 31 August 1981**

**Principal Investigator**

**Dr. Giuseppe Colombo**

**Co-Investigators**

**Dr. Mario D. Grossi  
Mr. David Arnold  
Dr. M. Martinez-Sanchez**

## INTRODUCTION

This report covers work done during the period 1 March through 31 August 1981 on two extensions of NASA Contract NAS8-33691. Section I, describes work done at SAO on the study of tether safety issues. Section II, describes the work done at MIT studying the use of tethers for payload orbital transfer.

## I. Study of Tether Safety Issues

This section presents a summary of work done at SAO on the study of tether safety issues. Detailed results are presented in the monthly reports for the period March - July, 1981. The effort during this period has been directed toward understanding the behavior of the tether after a failure at various distances from the Shuttle and after jamming of the reel mechanism during deployment. Analytic expressions derived under simplifying assumptions have been used to estimate the amount of recoil of the wire after a break as a function of the system parameters.

Since the first experiment with the Shuttle may be an electrodynamics experiment with a short tether, we have used the following test case for the studies. We assume a 100 metric ton Shuttle in orbit at 220 km with a 300 kg subsatellite deployed upward on a 10 km tether 2 mm in diameter. The wire is represented by discrete masses at 1 km intervals. Initial conditions have been computed such that the system is in equilibrium. A break in the wire is simulated by omitting the mass points representing the subsatellite and the portion of the wire beyond the break in the integration of the equations of motion. Runs have been done using 1, 2, and 5 of the masses representing the wire, plus the mass representing the Shuttle.

The case with only one wire mass can be described quite well without the use of numerical integration. From the tension in the wire, and the other parameters of the system we can calculate the velocity with which the mass point will recoil. Assuming that loss of tension between the wire mass point and the Shuttle occurs in a relatively short time, the initial position and velocity (consisting of the orbital velocity and the recoil velocity toward the Shuttle) can be used to calculate the new orbital elements for the wire mass point which now orbits as a free particle. From these orbital elements, the closest approach to the Shuttle and the time of closest approach can be calculated. A small computer program has been written using the analytic expressions in order to do a parametric study for breaks at various positions along tethers of various lengths. A table of results obtained is given in the monthly report for June, 1981. Two features are apparent from the table. First, the amount of recoil is approximately inversely proportional to the length of the broken piece of wire. Second, the results scale with the length of the wire (assuming the tension is proportional to the length of the wire). That is, if a 1 km piece of wire broken from a 10 km wire recoils 11 meters, we can multiply all the numbers by 10 and get the result that a 10 km piece broken from a 100 km wire recoils about 110 meters.

The expression for the recoil velocity is interesting because it turns out to be independent of the length of the wire segment represented by the mass point. The expression is obtained by setting the kinetic energy of the wire mass equal to the energy stored in the stretched piece of wire. The mass of the wire point is the product of the wire density, cross section, and length. The stiffness of the wire segment is the product of the elasticity, cross section, and the inverse of the length. Performing the algebra gives the expression

$$v_r = T/A\sqrt{\rho E}$$

where  $v_r$  is the recoil velocity,  $A$  is the wire cross section,  $\rho$  is the density, and  $E$  is the elasticity. The recoil can be reduced by making the wire thicker, or using materials with a higher density or stiffness. This formula was derived treating the wire as a single lump. Multi-mass runs are required to study the behavior of the wire in more detail.

The fact that the length of the wire segment does not appear in the expression for the recoil velocity suggests the possibility that all parts of the wire recoil with the same velocity. When a break occurs, the loss of tension will propagate down the wire at the speed of sound which is given by the expression  $\sqrt{E/\rho}$ . For the parameters used in the simulation this velocity is about 5.3 km/second. A run has been done with 5 wire mass points plus the Shuttle to see the behavior of the wire in more detail after a break. Detailed results are presented in the monthly report for July, 1981. The tension as a function of time is shown in Figure 2a. It takes about 1 second for the loss of tension to propagate down the 5 km wire. After the initial loss of tension, the various sections go in and out of tension as seen in the latter part of the plot. All sections of the wire acquire a velocity toward the Shuttle of about 30 cm/sec except for the point closest to the Shuttle. The behavior of the last point is anomalous, presumably because of boundary effects. The wire appears to move more or less as a unit after the break.

Because of the gradient of the gravitational and centripetal accelerations there is a stretching force acting on the wire. In a run done with only two wire mass points, the two masses moved toward each other in the initial contraction after the break until the stretching forces halted the motion and brought the masses back into tension. The masses bounced back and forth from each other in a cyclic fashion during the run. The run with five masses described previously exhibits the same behavior in a more complicated fashion. Basically, the wire contracts after the break to approximately the natural length of the wire, and then the distances between mass points oscillate around the natural length with different sections going in and out of tension. The wire as a whole moves toward the Shuttle with the recoil velocity given by the equation presented earlier.

Without atmospheric drag, coriolis forces cause the wire to move forward when the wire recoils (for upward deployment). The radial vs in-plane behavior for the run with five wire mass points plus the Shuttle is shown in Figure 2b. The in-plane motion is greatly exaggerated in the plot. Runs have been done for 2 wire mass points with, and without drag to see which effect dominates in this particular case. The motion without drag was about .9 meters forward after 60 seconds, and about 2.8 meters to the rear when drag was applied, indicating that drag dominates by a few factors in the case.

Two runs have been done to study the behavior of the wire in the case where the reel jams during deployment. Integrating the motion of only the subsatellite and the Shuttle with the wire considered massless gives a tension which increases to a maximum value and then falls to zero as the subsatellite recoils toward the Shuttle. The break strength of the 2 mm kevlar wire was not exceeded with a 20 m/sec deployment velocity and a 300 kg subsatellite. An analytic calculation shows a closest approach of 5.5 km to the Shuttle with the reel jam occurring at 10 km from the Shuttle. The run was repeated adding 4 wire mass points. Details of this run are given in the monthly report for July, 1981. Tension variations from 114 to 230 kg are seen along the wire as a result of the oscillations caused by the reel jamming. After the recoil, the sections of wire remain out of tension. Examination of the velocities of the various mass points shows the recoil velocity to be roughly proportional to the distance from the Shuttle. The wire is therefore continuing to contract on itself in contrast to the behavior seen in a break where the wire recoils with a nearly uniform velocity. More details of the reel jamming case will be presented in the next monthly report.

The figures from Monthly Report No. 4 are shown in the following pages as a summary of the study of the cases of a broken wire and jamming of the reel during deployment.

## Figure Captions

Figure 1. Radial vs in-plane component(cm) after a break 5 km from the Shuttle plotted every second for the first 18 seconds.

Figure 2. Simulation of a break 5 km from the Shuttle plotted every .1 seconds. Part a) is the tension(dynes) vs time(sec). Part b) is the radial vs in-plane component(cm).

Figure 3. Motion of the wire after a break 5 km from the Shuttle. In part a) the initial value of the radial component for each mass has been subtracted from the subsequent values and the curves have been separated from each other by 100 cm. Part b) is the modified radial component vs the in-plane component.

Figure 4. Motion in the radial direction after a break 5 km from the Shuttle. The values plotted were obtained by first subtracting the initial value for each mass, then subtracting the values for a reference mass from all the masses, and finally separating the curves by 35 cm. In part a) the sixth mass is used as the origin, and in part b) the second mass is used as origin.

Figure 5. Behavior of the wire after a break at 5 km with the first .8 seconds excluded from the plots. In part a) the value at .8 seconds is subtracted from each point, then the values for the second mass are subtracted from each curve, and finally the curves are separated by 2 cm. The value of the sixth component which is anomalous is essentially ignored by holding it fixed at the value of the separation constant. Part b) shows the tension vs time after .8 seconds.

Figure 6. Tension vs time after a reel jam with the subsatellite at 10 km being deployed at 20 m/sec. In part a) the mass of the tether is neglected. Part b) shows the tension for each wire segment with wire masses every 2 km along the wire.



ORIGINAL PAGE IS  
OF POOR QUALITY

MASS SYMBOL

1	⊖
2	△
3	+
4	×
5	◇
6	⬆

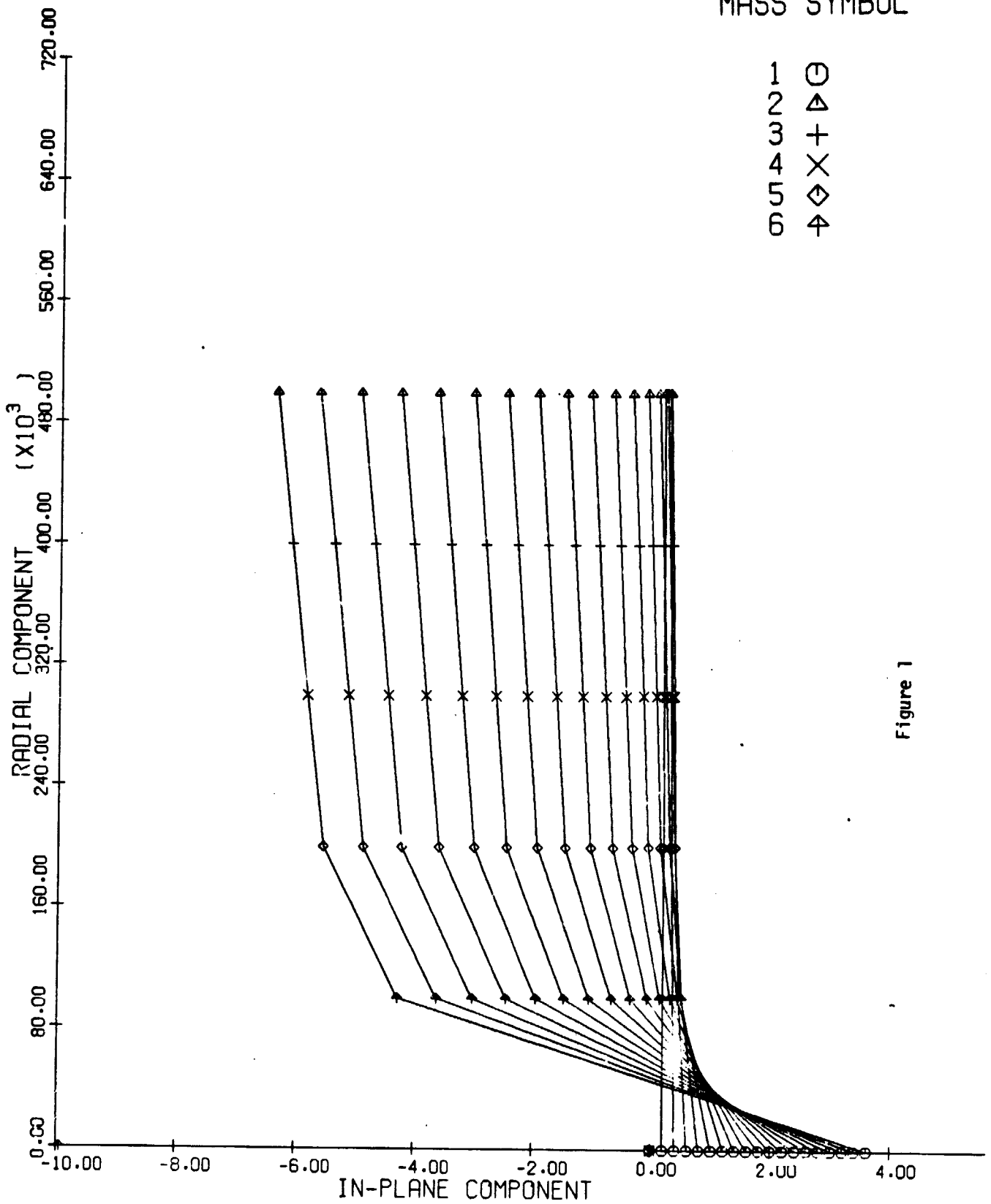


Figure 1

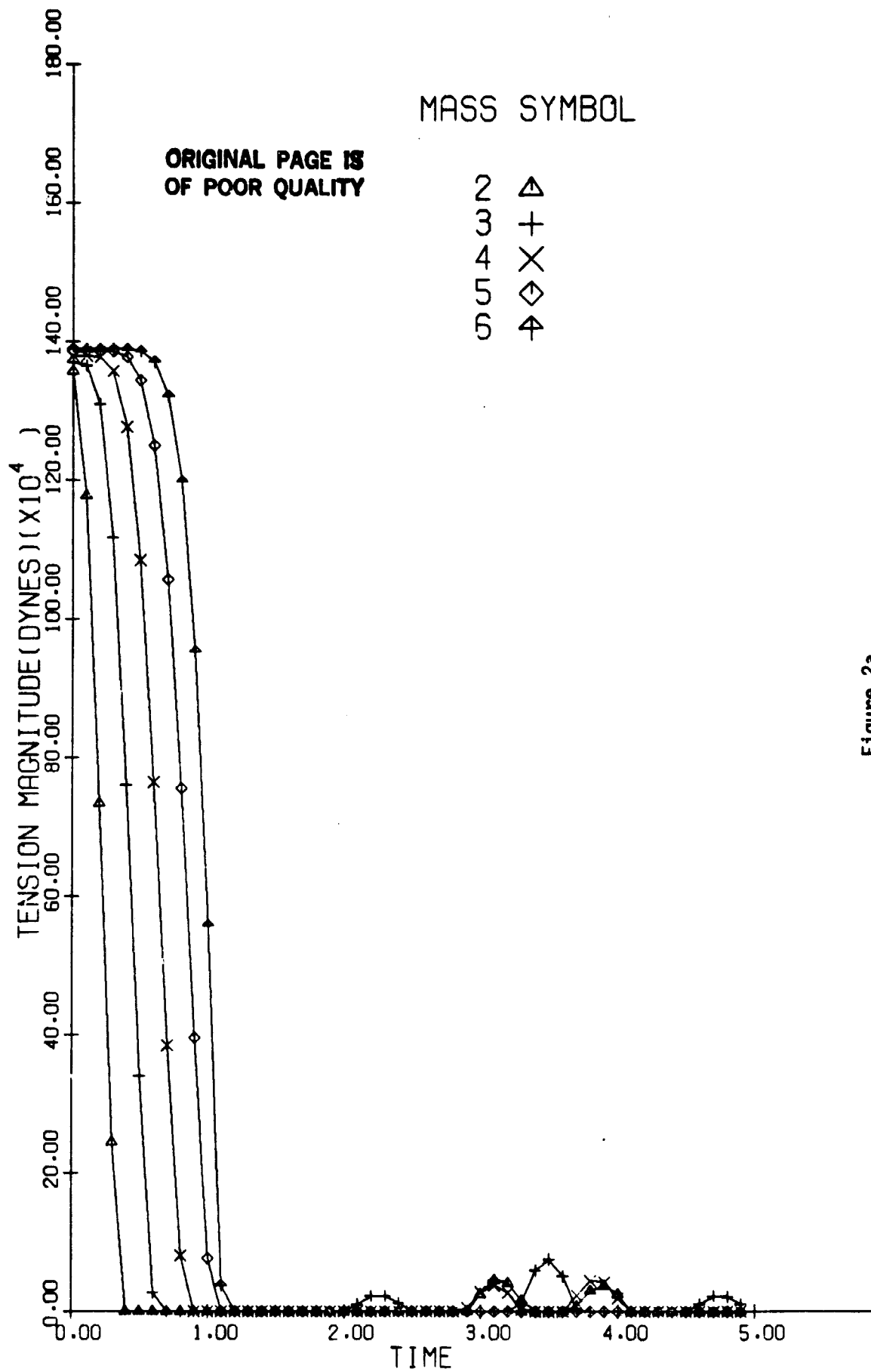


Figure 2a

ORIGINAL PAGE IS  
OF POOR QUALITY

MASS SYMBOL

1	○
2	△
3	+
4	×
5	◇
6	⋈

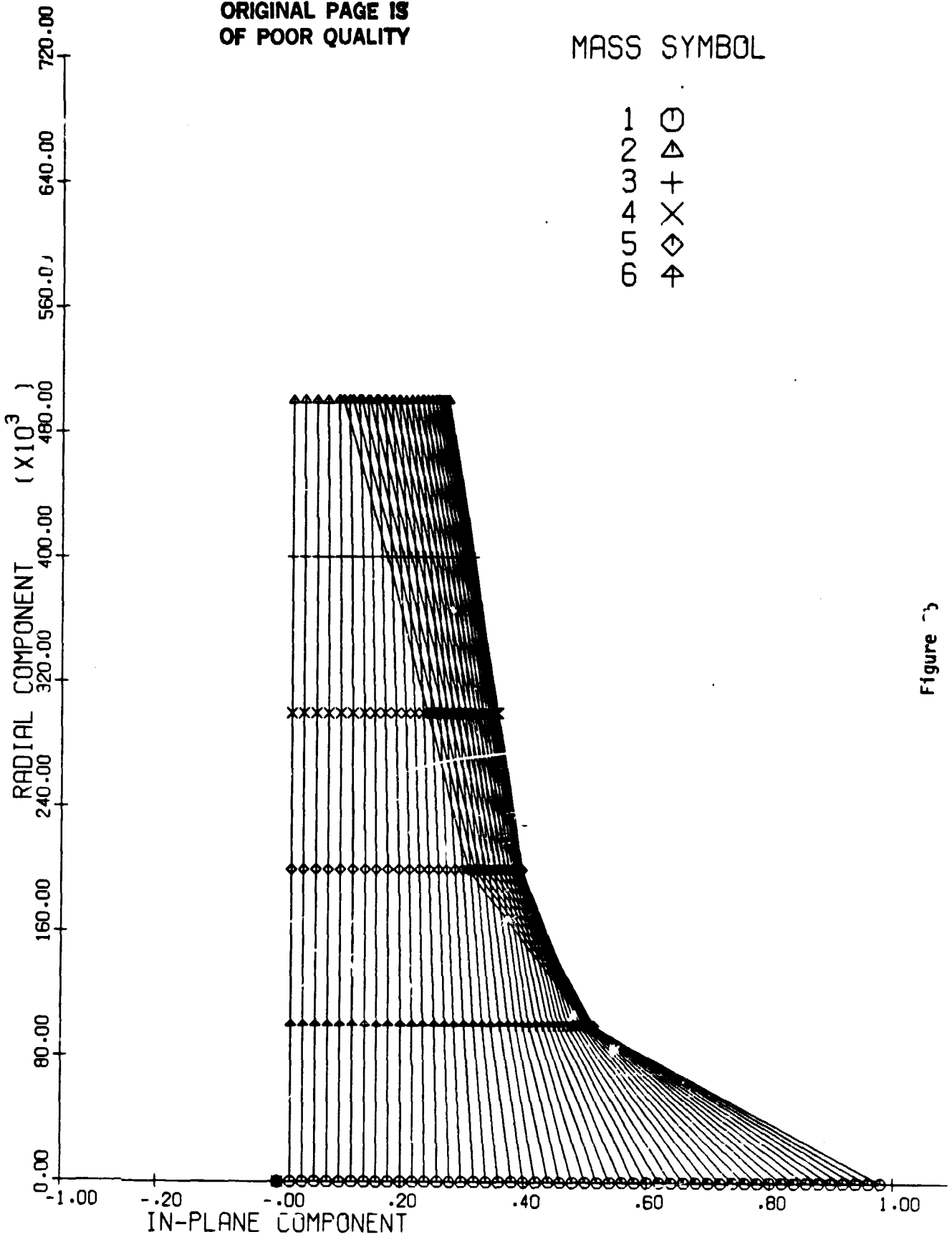


Figure 3

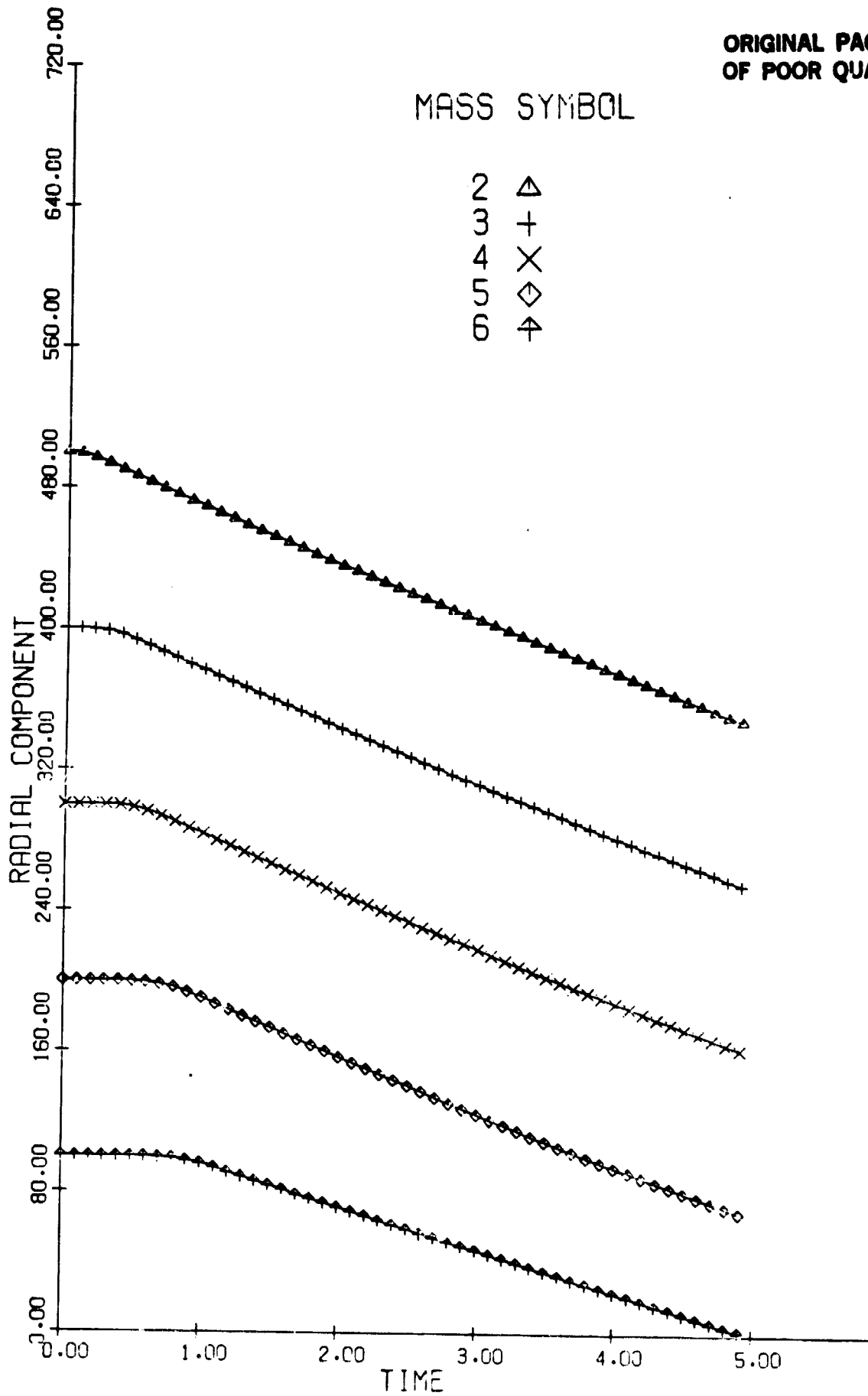


Figure 3a

ORIGINAL PAGE IS  
OF POOR QUALITY

MASS SYMBOL

1	○
2	△
3	+
4	×
5	◇
6	↑

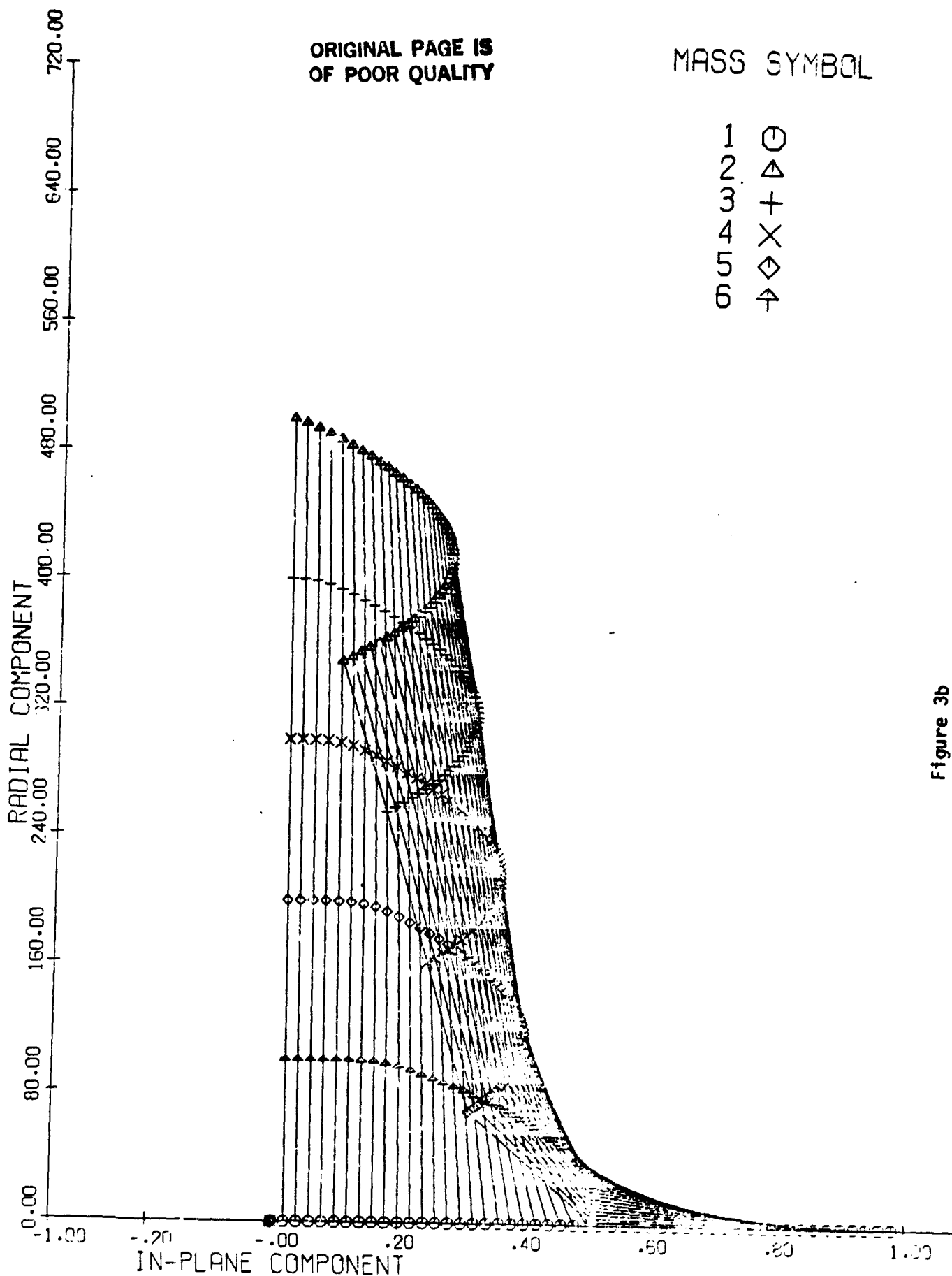


Figure 3b

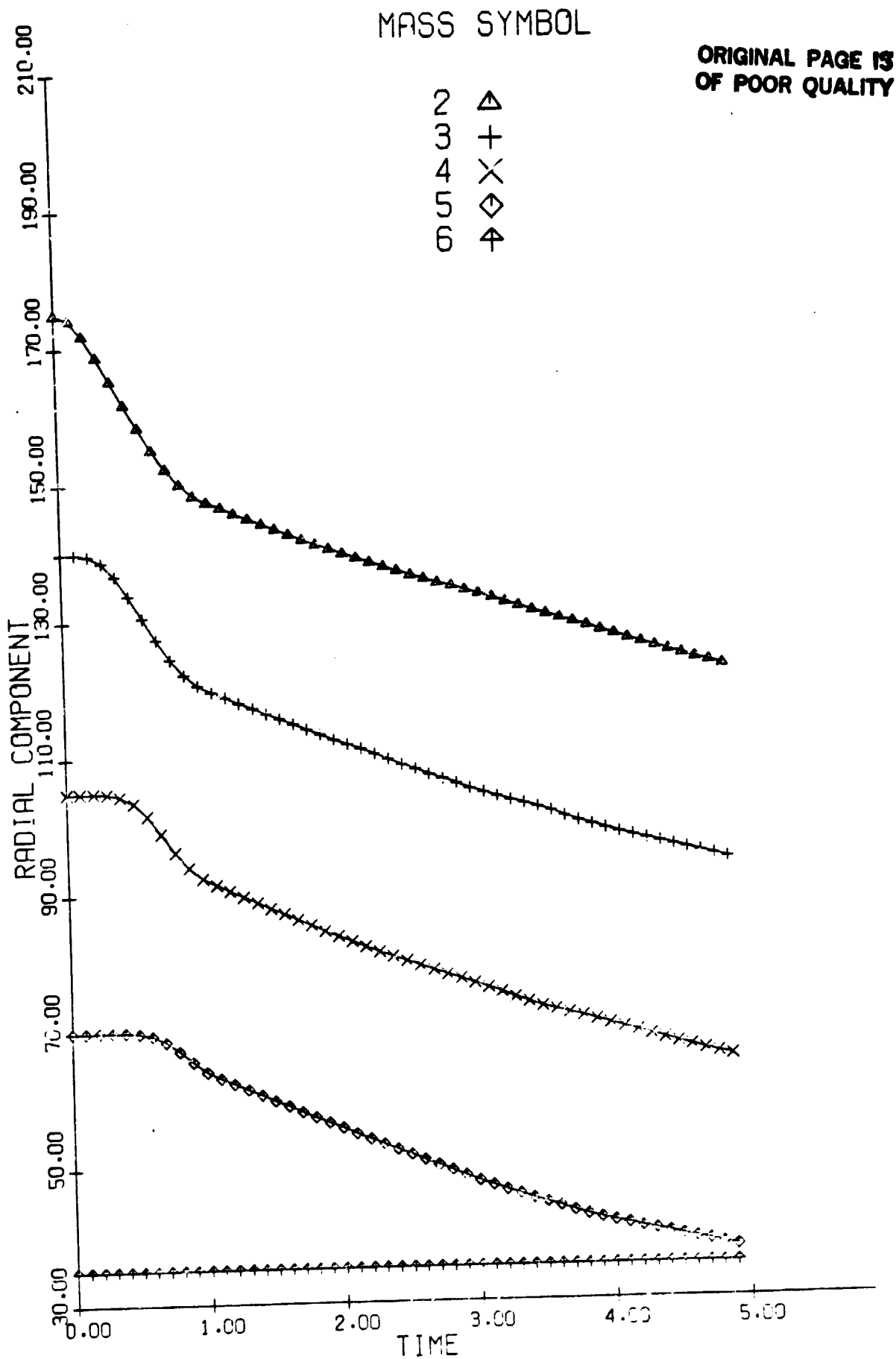


Figure 4a

# MASS SYMBOL

ORIGINAL PAGE IS  
OF POOR QUALITY

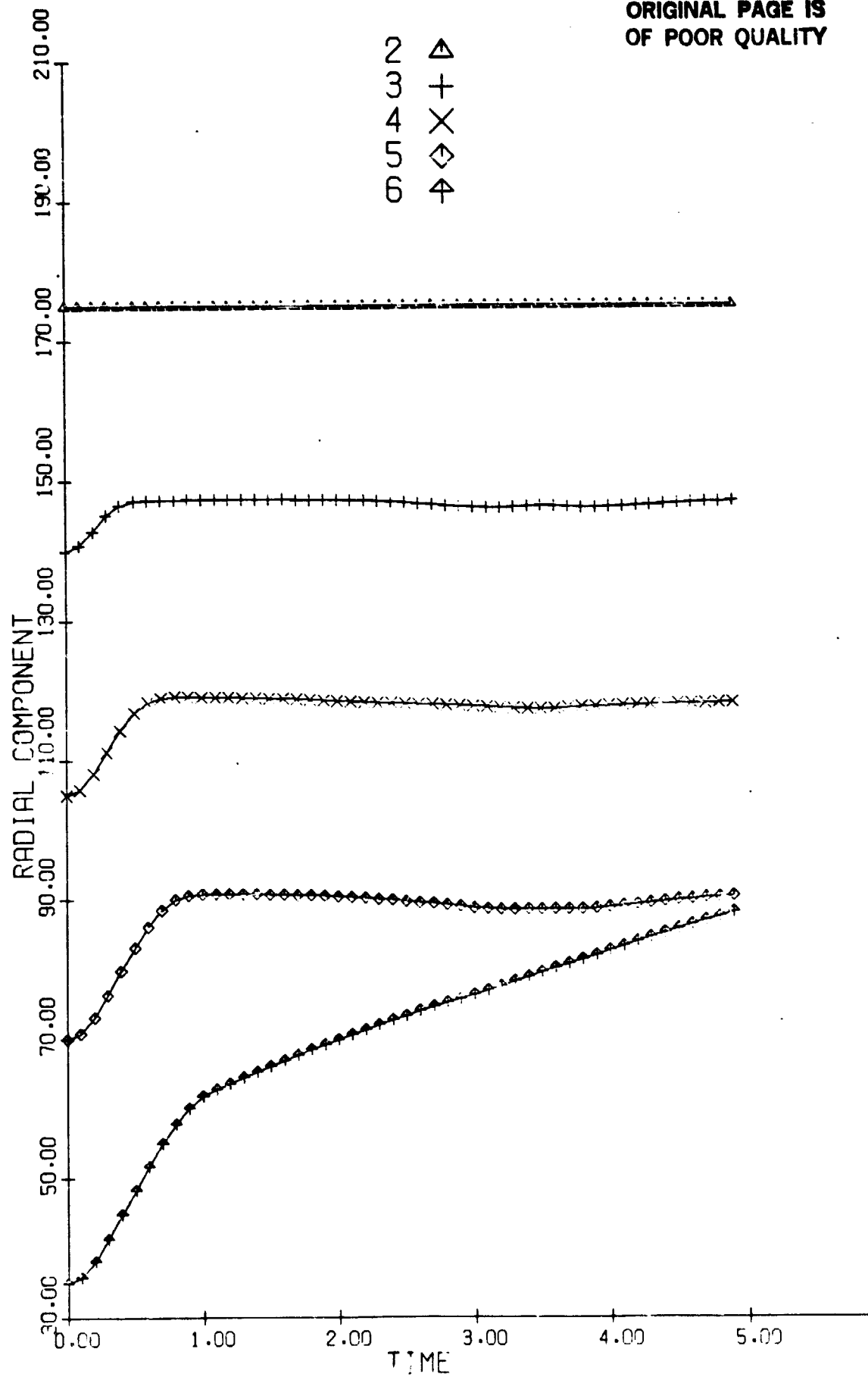


Figure 4b

ORIGINAL PAGE IS  
OF POOR QUALITY

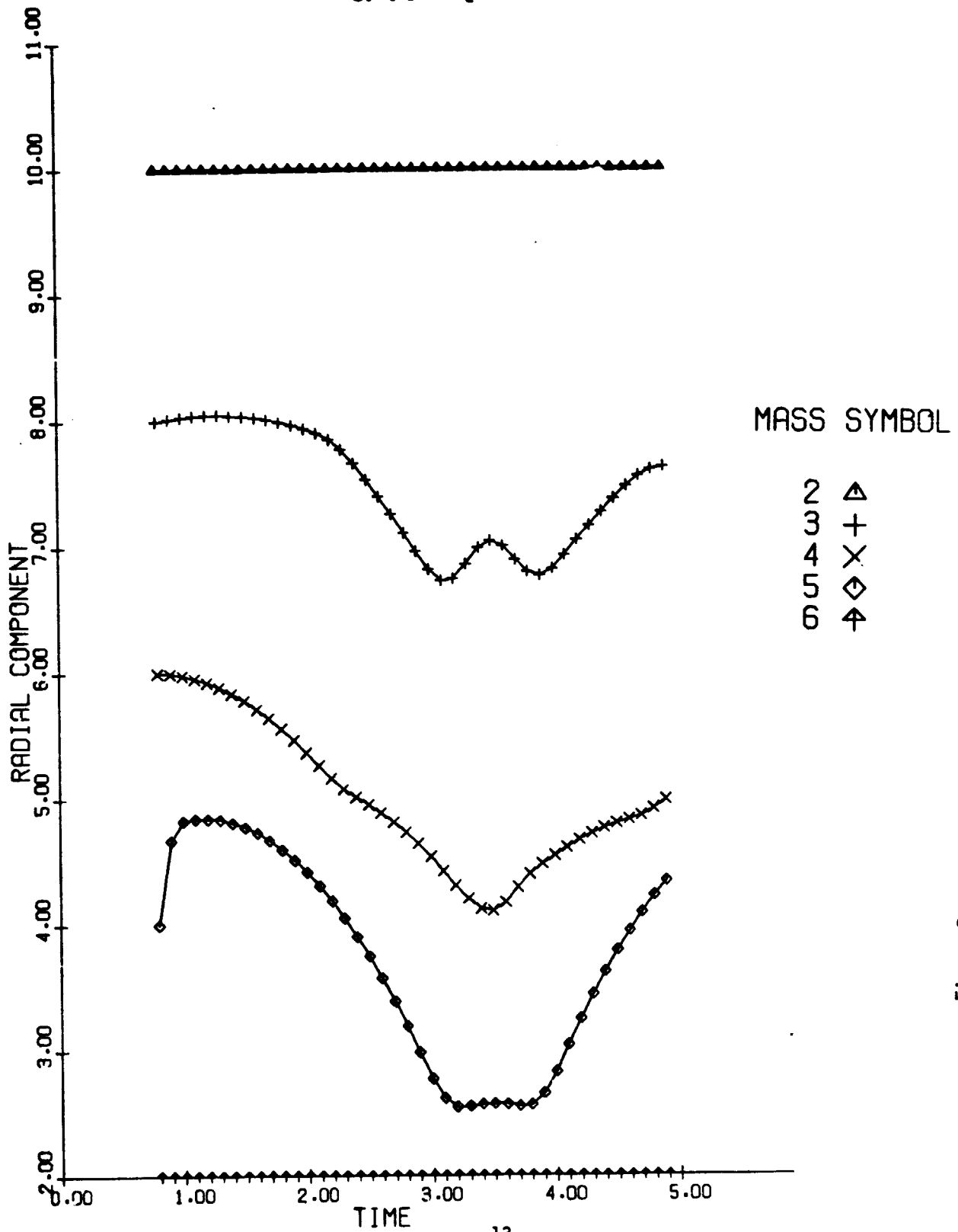


Figure 5a



ORIGINAL PAGE IS  
OF POOR QUALITY

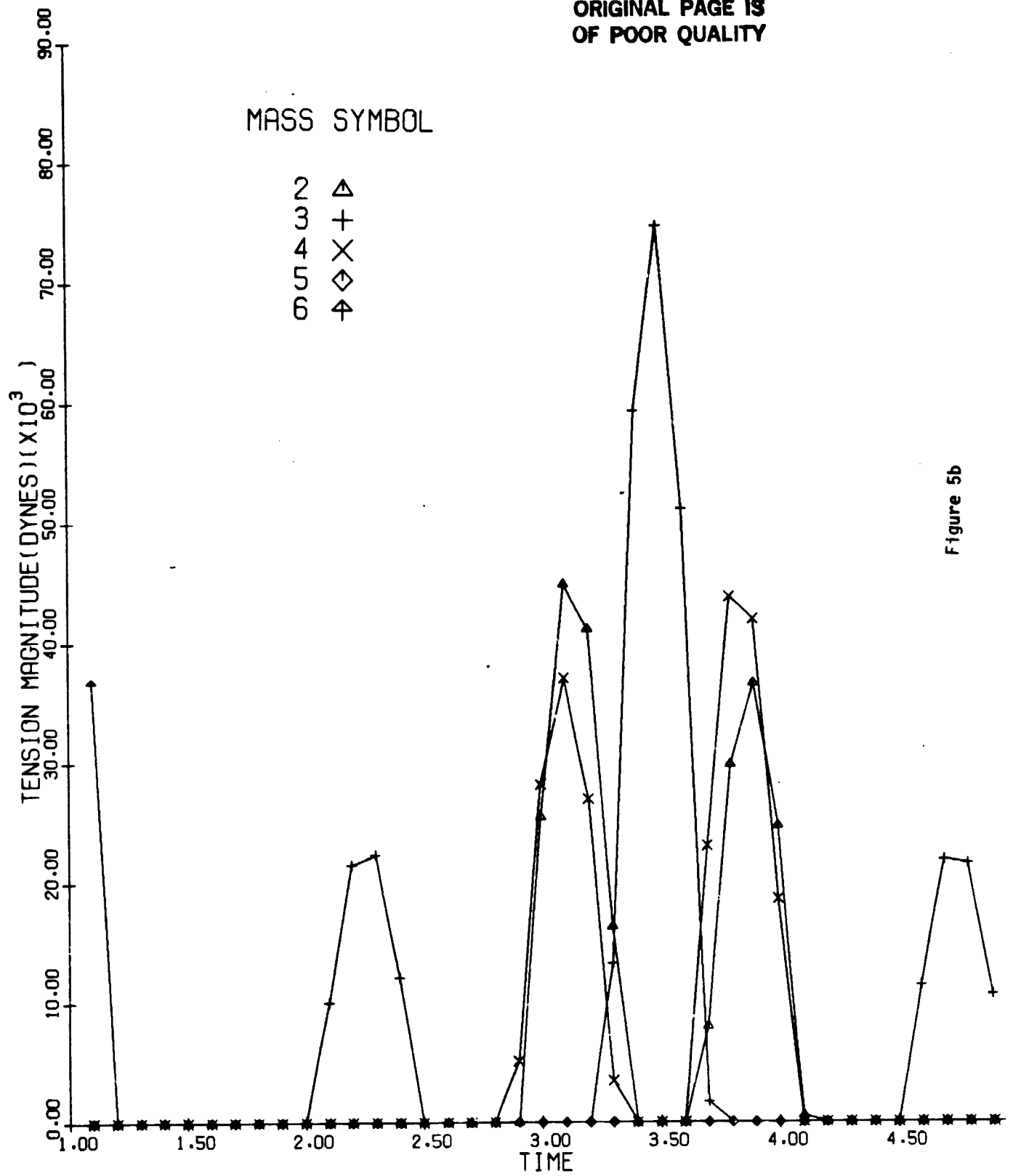


Figure 5b

ORIGINAL PAGE IS  
OF POOR QUALITY

MASS SYMBOL

2  $\Delta$

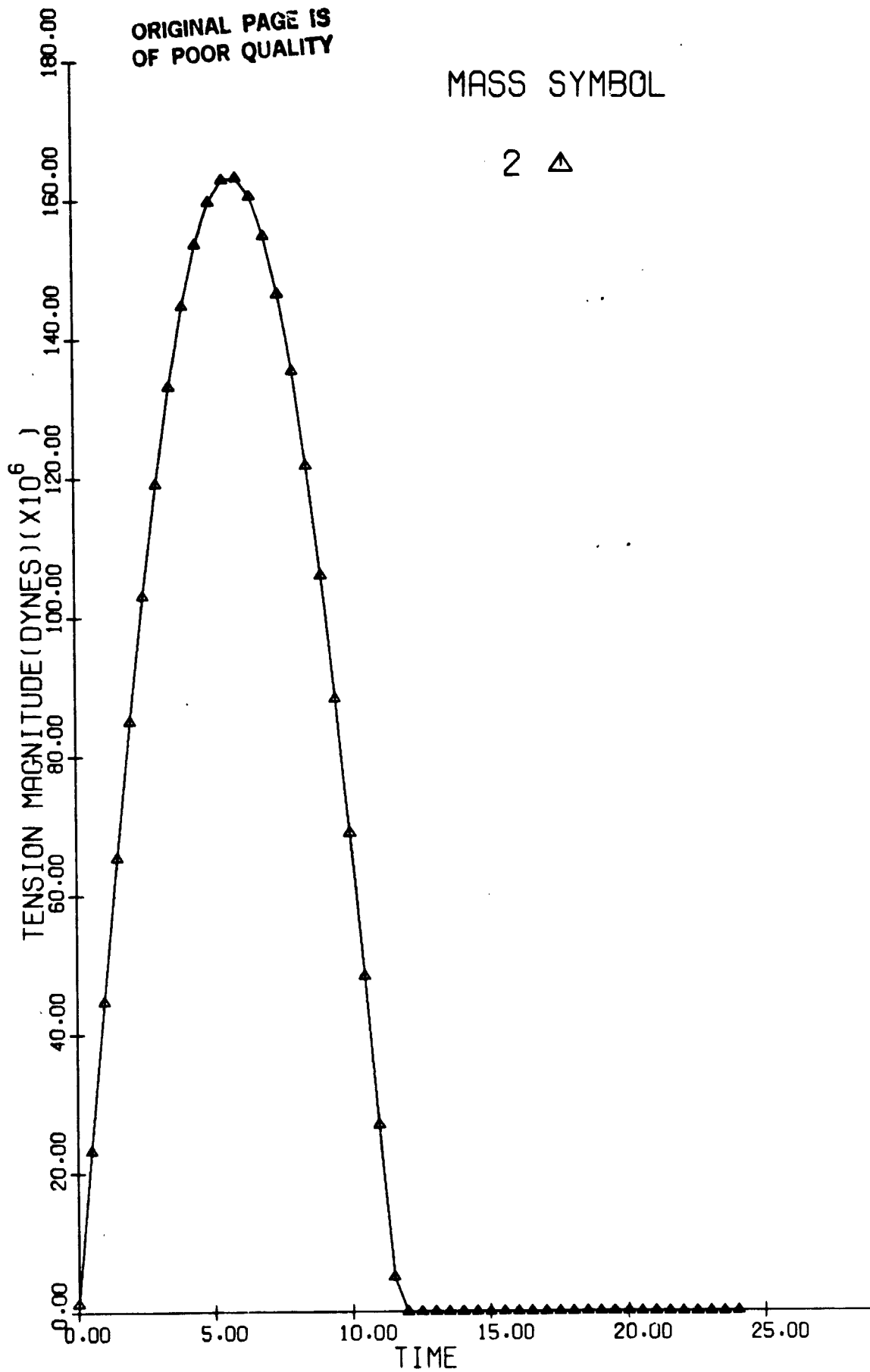


Figure 6a

ORIGINAL PAGE IS  
OF POOR QUALITY

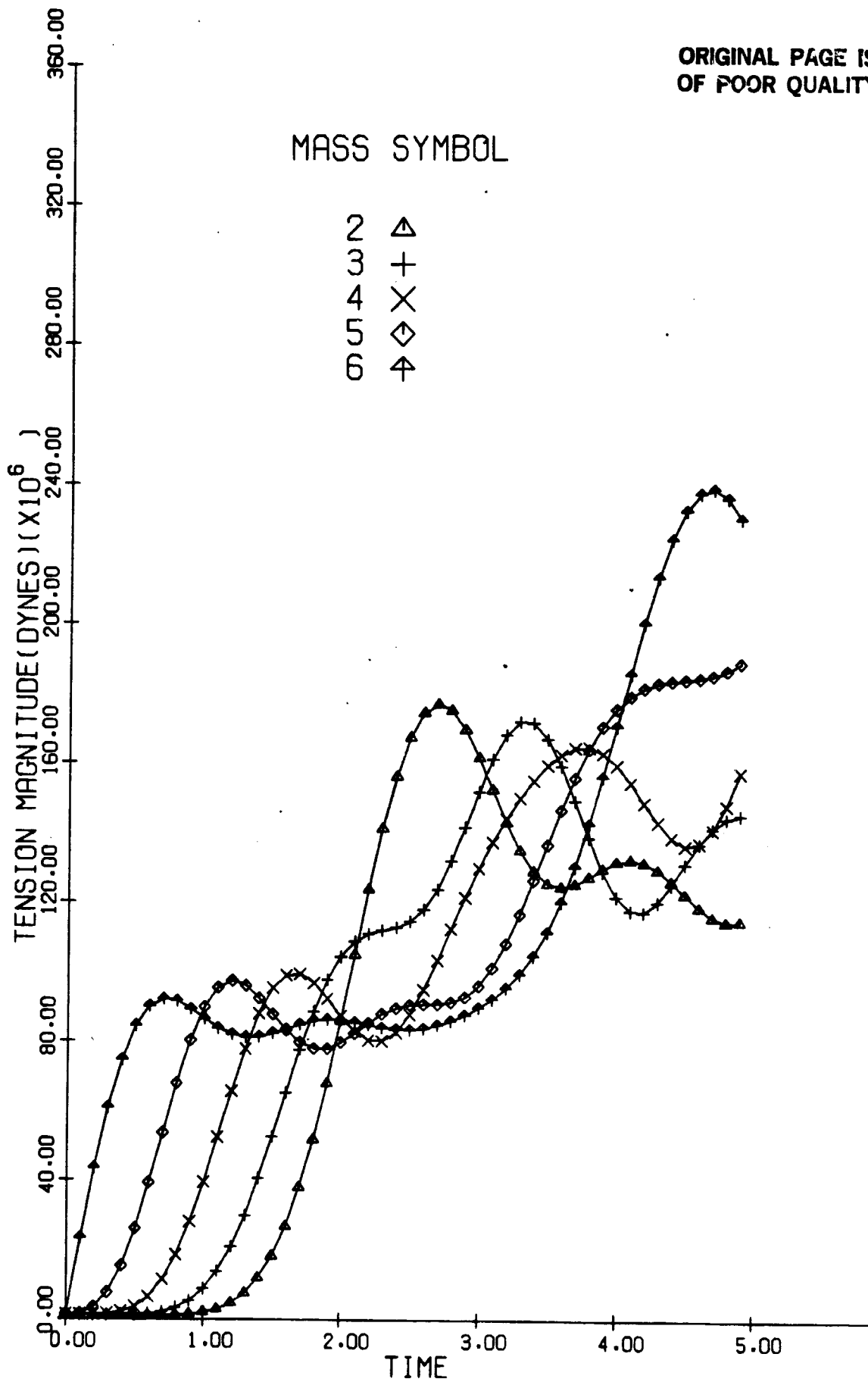


Figure 6b

## **ACKNOWLEDGEMENT**

**The authors of this report are Mr. D.A. Arnold and  
Dr. M. Martinez-Sanchez.**

## II. The Use of Tethers for Payload Orbital Transfer

### Introduction

During this first reporting period the work has centered on our first task namely, the selection of concepts for orbit transfer missions which show promising improvements by the use of tethers.

A preliminary look at the original MTPF concept (a Shuttle-based tether system flown to and from orbit in each Shuttle flight) indicated only marginal benefits. The alternative concept was then evolved of a free-flying tether system, deployed in a first flight, then left in orbit for docking with successive payload-carrying Shuttle flights. Significant payload increases were found if this device is used for LEO-GEO transfers, in a mode where the payload carries a propulsion stage (IUS or Centaur) for first  $\Delta V$  assist and for the circularization  $\Delta V$  in GEO.

A more ambitious system was also examined in which a second tethered system in GEO takes the role of providing the circularization step. Particular attention was paid to the requirement that the transfer duration should be a rational fraction of one day, to provide additional encounters in case of rendezvous failure. It was found that for most combinations of parameters, the length of the upper tether ranged around 10,000 Km, while the one in LEO was about 1,000 Km. Progressive addition of  $\Delta V$  capabilities at the two ends of the transfer can, of course, reduce these lengths.

Operational limitations based on minimum perigee height and maximum tether weight were studied.

A preliminary conclusion of this work has been that operating modes which combine tether assist with substantial rocket-derived velocity increments can be of importance in increasing the payload deliverable to high and geosynchronous orbits, or for escape. This capability may be crucial for certain missions, such as the Galileo mission, which are at the edge of the Shuttle's capabilities.

Single tether concepts for orbit transfer.

Use of a tether facility as a permanent facility of the Shuttle does not appear justified for missions that fall within the operational envelope of the orbiter with its integral OMS tanks. This is because, even though the tether allows deployment of the payload from a lower Shuttle orbit (typically an elliptic one), the payload cannot be increased due to other constraints, such as payload bay structural integrity and c.g. location. The only savings are then in the use of less OMS fuel, but these cannot balance the loss of revenue from the payload displaced by the tether itself. An example is shown in Table 1: a 47 km tether allows payload to be placed in a 500/500 Km orbit from a Shuttle in a 185/453 Km orbit, with an OMS fuel savings of \$33,000. However, the mass and length of the tether facility displaces payload worth \$2.80 M. Similar results are shown for a polar orbit.

There are some possible scenarios where a Shuttle based tether could be cost-effective. These refer to low Earth orbits high enough (particularly for polar orbits) that payload is limited by OMS fuel capacity, including extension kits. A trade-off study is planned to determine how far the operating envelope can be extended by a permanent Shuttle tether.

TABLE 1.

## COST TO LOW ENERGY MISSION\*\*

	<u>Space Telescope</u>	<u>Polar Orbit</u>
	Orbit 500km/28.8°	1000 km/97°
Weight of Payload (kg)	11,000	3,000
Length of Payload (m)	13.1	9.0
Diameter of Payload (m)	4.26	
Cost to current Shuttle (\$M)	20.20	23.07
Cost to Shuttle + Orbiter based tether system (\$M)	23.00	29.8
Lost revenue from displaced payload (\$M)	-2.80	-6.73
OMS fuel savings (\$M)	(0.033)	(0.083)
Benefit of using tether system (\$M)	-2.77	-6.647

\*\*

1) Cost per Shuttle flight = \$27.3 at ETR

\$46.9 at WTR

2) Elliptic shuttle orbit + tether transfer  
perigee altitude = 185 km

TABLE 2.

## PAYLOAD BENEFIT FOR GEOSYNCHRONOUS ORBIT TRANSFER\*

Tether length (km)	Payload Weight (kg)	Payload increase (%)
0	2465	
100	3122	18
200	3675	39
300	4326	63
400	5100	93

## \*Calculation conditions:

## 1. SHUTTLE + Two stage IUS

Stage	1	2
Isp(sec)	291.9	289.7
f stru.	.946	.933
WT prop.(kg)	9707	(2722)

## 2. Parking orbit: 300/300 km

## 3. Tether system dock with shuttle in parking orbit.



TABLE 3.

## PAYLOAD BENEFIT FOR SOLAR SYSTEM EXPLORATION\*\*

C3 (km <sup>2</sup> /sec <sup>2</sup> )	Tether length (km)	Injected mass (kg)	Increase (%)
15	0	7693	
	100	8253	7.2
	200	8857	15
	300	9511	23.6
	400	10219	32.8
<hr/>			
80	0	2246	
	100	2413	7.4
	200	2589	15.2
	300	2771	25.3
	400	2963	31.9

\*\* Calculation conditions:

1. SHUTTLE + CENTAUR

Isp = 444 sec

WT of propellant = 13608 kg

Dry WT = 1827 kg

2. Parking orbit: 300/300 km

3. Tether system dock with shuttle in parking orbit.

4.  $C_3 = v^2 - \frac{2 \mu_e}{r}$

It appears, however, that a more efficient system would be, in any case, one where the tether and its end platforms would be left deployed in space, to be docked with the Shuttle each time. The Shuttle would transfer the payload (possibly with a transfer propulsion stage attached) to the tether lower platform; the payload would then move to the upper platform, be released, and the Shuttle would then detach and reenter. The problem of re-establishing the initial orbit for the tether has to be examined in more depth; some of the required propulsion could be provided by the Shuttle itself, but the fact that the platform stays in space opens the possibility of using substantial amounts of high specific impulse electric propulsion in the process. Thus, the system becomes a hybrid between the original TOTF (Tethered Orbital Transfer Facility) and the MTPF (Mechanized Tether Platform Facility) concepts, with the platform mass being a parameter to be optimized.

A preliminary examination of the performance gains for this free-flying tether concept was made, and is shown in Tables 2 and 3. Particularly for transfer to geostationary orbits, large payload increases are shown to be possible with tether lengths not exceeding 400 Km. Orbital perturbation during ascent (with the associated minimum perigee problem) and orbit reestablishment, as discussed, remain to be studied in more detail.

#### Two-tether LEO-GEO systems.

The principal interest in orbital transfer relates to low-to-geosynchronous cases. We considered the possibility of performing such transfers without any transfer propulsion, or with small  $\Delta V$ 's at most. This

requires a tether to be attached to a low Earth orbiting platform for release into the transfer ellipse, and another tether attached to a geosynchronous platform, to acquire the payload and circularize its orbit.

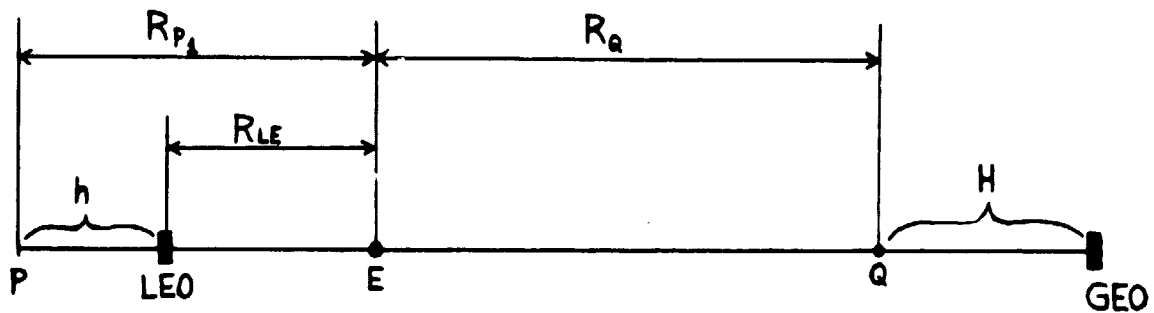


FIGURE 1. Geometry for a two-tether system.

The length  $H$  of the upper tether depends only upon the period  $P_2$  chosen for the orbit of the payload (after application of an apogee velocity increment  $\Delta V_Q$ ). This is because two elements of that orbit are prescribed, namely, the semimajor axis (by the period) and the angular momentum (by the requirement that the angular velocity at apogee must equal that in the geosynchronous orbit). These conditions can be expressed as

$$P_2 = \frac{2\pi}{\sqrt{\mu_e}} \left( \frac{R_{P_2} + R_Q}{2} \right)^{3/2} \quad (1)$$

(where  $R_{P_2}$  is the perigee of the orbit and  $\mu_e$  the gravitational constant of Earth) and

$$v^2(\text{apogee}_2) = \mu_e \left( \frac{2}{R_Q} - \frac{2}{R_{P_2} + R_Q} \right) = v_{GS}^2 \left( \frac{R_Q}{R_{GS}} \right)^2 \quad (2)$$

where the subscript GS refers to the geosynchronous orbit. Using

$v_{GS}^2 = \mu_e / R_{GS}$ , Eqs. (1) and (2) can be combined by elimination of  $R_{P_2}$  to give

$$\frac{2 \left( \frac{R_Q}{R_{GS}} \right)}{2 - \left( \frac{R_Q}{R_{GS}} \right)^3} = \frac{2}{R_{GS}} \left( \frac{\sqrt{\mu_e}}{2\pi} P_2 \right)^{2/3} \quad (3)$$

which can be solved for  $R_Q$  once  $P_2$  is prescribed. The tether length follows then from

$$H = R_{GS} - R_Q \quad (4)$$

and the perigee  $R_{p_2}$  from

$$R_{p_2} = \frac{R_Q^4}{2R_{GS}^3 - R_Q^3} \quad (5)$$

The subscript 2 has been used so far to indicate conditions after application of  $\Delta V_Q$ . For the ascent orbit (before  $\Delta V_Q$ ), the apogee velocity is

$$V(\text{apogee}_1) = V(\text{apogee}_2) - \Delta V_Q = V_{GS} \frac{R_Q}{R_{GS}} - \Delta V_Q \quad (6)$$

and Eq. (2) can be modified to calculate the perigee  $R_{p_1}$  of this ascent orbit:

$$\mu_e \left( \frac{2}{R_Q} - \frac{2}{R_{p_1} + R_Q} \right) = \left( V_{GS} \frac{R_Q}{R_{GS}} - \Delta V_Q \right)^2 \quad (7)$$

Once  $R_{p_1}$  is so determined, the velocity at perigee can be expressed (from conservation of angular momentum) as

$$V_{p_1} = \frac{R_Q}{R_{p_1}} V(\text{apo.}_1) = \frac{R_Q}{R_{p_1}} \left( V_{GS} \frac{R_Q}{R_{GS}} - \Delta V_Q \right) \quad (8)$$

This velocity contains, in general, a propulsion-derived increment  $\Delta V_P$ , applied at or immediately after release. The velocity of the end of the low-Earth tether is therefore

$$V_{\text{tether end}} = V_{p_1} - \Delta V_P \quad (9)$$

and the orbital velocity  $V_{C, LE}$  of the platform at  $R_{LE}$  (or, more precisely, of the orbital center of the tether-payload system) is therefore

$$V_{C, LE} = \sqrt{\frac{\mu_e}{R_{LE}}} = (V_{P_1} - \Delta V_P) \frac{R_{LE}}{R_{P_1}} \quad (10)$$

from which  $R_{LE}$  can be calculated easily. Finally, the low-Earth tether length is

$$h = R_{P_1} - R_{LE} \quad (11)$$

Fig. 2 and Table 4 show calculated results for the case of  $\Delta V_P = \Delta V_Q = 0$ . If we impose the requirement that, in case of docking failure, the payload and the lower platform of the GEO tether should rendezvous again after an integer number of orbits, then the period  $P_2$  (T in Fig. 2) must be a rational fraction  $m/n$  of a day ( $m, n$  integers). Thus, appropriate values of  $P_2$ , for low  $m$  and  $n$ , are

1/3 day = 8 hr., 3/8 day = 9 hr., 2/5 day = 9.6 hr., 1/2 day = 12 hr.

As shown in Fig. 2, a period of 1/3 day implies an upper tether length of over 10,000 Km, and a lower tether length of about 1200 Km from a low Earth orbit at 1200 Km as well. Increasing the period to 1/2 day lowers the length of the upper tether to about 6000 Km but it also requires the low Earth orbit to be at some 9000 Km altitude, with a 1600 Km tether.

ORIGINAL PAGE IS  
OF POOR QUALITY

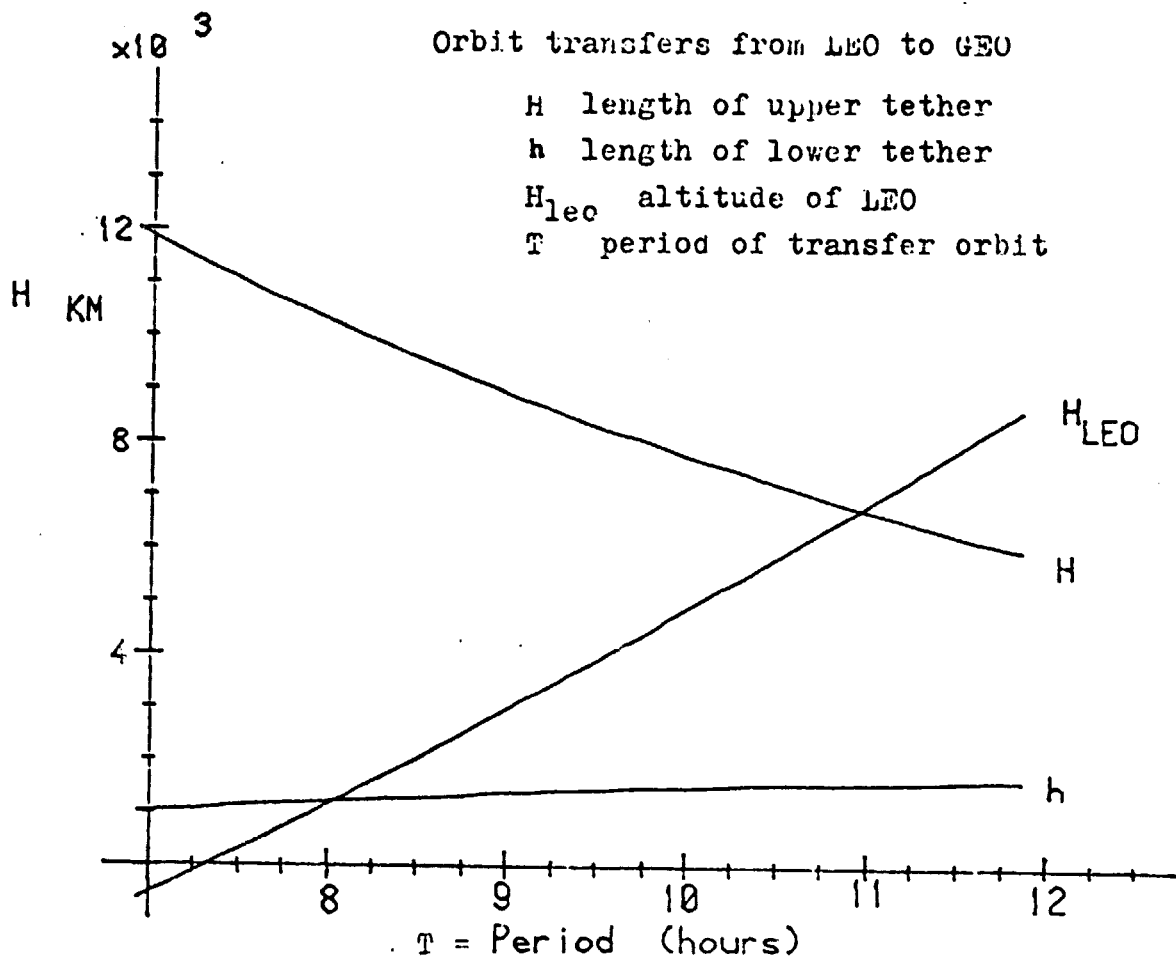


FIGURE 2. TWO-TETHER SYSTEM CHARACTERISTICS WITH  $\Delta V_P = \Delta V_Q = 0$ .

TABLE 4. TWO-TETHER SYSTEM CHARACTERISTICS WITH  $\Delta V_P = \Delta V_Q = 0$ .

H=	7000.000	T=	10.77674	H1=	1584.303	HLE0=	6402.393
H=	7250.000	T=	10.52514	H1=	1561.823	HLE0=	5900.962
H=	7500.000	T=	10.28163	H1=	1537.997	HLE0=	5419.849
H=	7750.000	T=	10.04582	H1=	1513.000	HLE0=	4958.085
H=	8000.000	T=	9.817351	H1=	1486.986	HLE0=	4514.776
H=	8250.000	T=	9.595901	H1=	1460.100	HLE0=	4089.070
H=	8500.000	T=	9.381143	H1=	1432.474	HLE0=	3680.165
H=	8750.000	T=	9.172782	H1=	1404.236	HLE0=	3287.299
H=	9000.000	T=	8.970538	H1=	1375.486	HLE0=	2909.765
H=	9250.000	T=	8.774145	H1=	1346.331	HLE0=	2546.881
H=	9500.000	T=	8.583347	H1=	1316.864	HLE0=	2198.010
H=	9750.000	T=	8.397913	H1=	1287.168	HLE0=	1862.546
H=	10000.00	T=	8.217616	H1=	1257.319	HLE0=	1539.918
H=	10250.00	T=	8.042239	H1=	1227.390	HLE0=	1229.577
H=	10500.00	T=	7.871587	H1=	1197.443	HLE0=	931.0140
H=	10750.00	T=	7.705462	H1=	1167.537	HLE0=	643.7385
H=	11000.00	T=	7.543689	H1=	1137.726	HLE0=	367.2815
H=	11250.00	T=	7.386090	H1=	1108.058	HLE0=	101.2060
H=	11500.00	T=	7.232506	H1=	1078.576	HLE0=	-154.9055
H=	11750.00	T=	7.082776	H1=	1049.318	HLE0=	-401.4575
H=	12000.00	T=	6.936757	H1=	1020.325	HLE0=	-638.8290

NOTE: H1 is equivalent to h, which has previously been used.



For a constant-stress tether (stress =  $\sigma$ , density =  $\rho$ ) extending from  $r_{LE}$  to  $R = r_{LE} + h$ , the area distribution is easily found to be

$$A(r) = A_{LE} \exp \left[ \frac{\mu_e \rho}{\sigma} \left( \frac{3}{2r_{LE}} - \frac{r^2}{2r_{LE}^3} - \frac{1}{r} \right) \right] \quad (12)$$

where  $A_{LE}$ , the thickest section, is found from equilibrium at the higher end, where a satellite of mass  $M_{sat}$  is attached:

$$M_{sat} \left( \frac{\mu}{3} \frac{R}{r_{LE}} - \frac{\mu}{R^2} \right) = \sigma A_{LE} \exp \left[ \frac{\mu_e \rho}{\sigma} \left( \frac{3}{2r_{LE}} - \frac{R^2}{2r_{LE}^3} - \frac{1}{R} \right) \right] \quad (13)$$

Most of the tether mass is concentrated near the lower end, where a good approximation to Eq. (12) can be obtained by series expansion of the exponent

$$A(r) \approx A_{LE} \exp \left[ - \frac{3}{2} \frac{\mu_e \rho}{\sigma r_{LE}} \left( \frac{r - r_{LE}}{r_{LE}} \right)^2 \right] \quad (14)$$

and this can be integrated to obtain an expression for the tether mass:

$$\frac{M}{M_{sat}} = \frac{2}{3} \sqrt{\frac{\pi}{2}} \frac{3+3\delta+\delta^2}{(1+\delta)^2} \gamma e^{\gamma^2 \frac{1+\delta/3}{1+\delta}} \operatorname{erf}(\gamma) \quad (15)$$

where

$$\delta = \frac{h}{r_{LE}}, \quad \gamma = \frac{h}{r_{LE}} \sqrt{\frac{3\mu_e \rho}{2\sigma r_{LE}}} \quad (16)$$

For  $\delta \lesssim 0.2$ ,  $M/M_{sat}$  is seen to depend mostly on the nondimensional group  $\gamma$  (Eq. (16)). For  $\delta$  in the vicinity of 0.2 ( $h \approx 1350$  km), the variation is shown in Table 5 below.

Table 5. Approximate tether mass

$\gamma$	0	0.1	0.2	0.4	0.6	0.8	1	1.2	1.6	2	2.5	3
$M/M_{sat}$	0	.02397	.09748	.4172	1.0539	2.2148	4.3293	8.2974	32.112	147.59	1365.3	18.898

For Kevlar,  $\gamma \sim 10 \frac{h}{r_{LE}}$  (about 2 for  $H = 1200$  Km). Thus, for payloads of the order of 10 Tonne, unreasonably heavy tether lines are obtained. However, the exponential nature of the  $M(h)$  function indicates rapid mass reductions if the lower tether length can be reduced by application of moderately small  $\Delta V$ 's.

For the mass of the upper tether, Eqs. (15), (16) still applies if the sign of  $\delta$  is reversed;  $r_{LE}$  is replaced by  $r_{GS}$  and  $h$  is replaced by  $H$ . The effective new value of  $\gamma$  is then of the order of 1.1, which indicates a moderate tether mass, of the order of 8 times that of the payload itself. Thus, despite the much greater length of the GEO tether, it is the one in LEO that needs substantial reduction.

The effect of introducing both perigee and apogee firings ( $\Delta V_p$  and  $\Delta V_a$ , respectively) was next investigated. The results for a wide range of parameters are listed in Tables 6 through 9. For the cases of the 1/3 and 1/2 day period, the results are also displayed graphically in Figs. 3 and 4. The effects are generally as follows:

- (a) Increasing  $\Delta V_p$  at constant period increases the altitude of LEO, and decreases the lower tether length,  $h$ .
- (b) Increasing  $\Delta V_Q$  at constant period decreases the altitude of LEO. For low  $\Delta V_p$ , increases of  $\Delta V_Q$  result in a shorter lower tether, but the reverse is true at high values of  $\Delta V_p$  ( $\geq 800$  m/sec).
- (c) As discussed before, the length  $H$  of the upper tether is unaffected by either  $\Delta V_p$  or  $\Delta V_Q$ , but is reduced if the period is allowed to increase.
- (d) For each transfer time and each value of  $\Delta V_p$ , there is a maximum  $\Delta V_Q$  for which the lower Earth orbit becomes too low (a limit of 200 Km was assumed here). Similarly, for each  $\Delta V_Q$ , there is a minimum  $\Delta V_p$  for the same reason.
- (e) The length of the lower tether can be reduced to zero by increasing  $\Delta V_p$  for each  $\Delta V_Q$ . The effect of  $\Delta V_Q$  on  $h$  is minor.

As an example of a combination which could be useful, we see in Fig. 4 that, from a 500 Km LE orbit, using a lower tether of length 390 Km and supplying a velocity increment  $\Delta V_p \approx 1500 \frac{\text{m}}{\text{sec}}$  after release, a payload can be put into a transfer ellipse leading to capture by the lower end of a GEO tether of 5913 Km length, if an apogee velocity increment  $\Delta V_Q \approx 725$  m/sec is applied prior to docking. If docking fails, another attempt can be made after one day (two orbits of the payload). Notice that for this lower tether length, its mass can be of the order of the payload mass.

**TABLE 6. TRANSFER TO GEO BY TETHER, WITH  $\Delta V$ 's SUPPLIED BY PROPULSION**

T = 1/3 day

Upper Tether Length: H = 10,322 km

$\Delta V_P$	$\Delta V_Q =$ 0	100	150	175	200	225	m/s		
0	1218 1138	1142 297							
300	1035 1321	990 449							
600	841 1515	829 610							
900	633 1723	659 780	663 347						
1200	412 1944	477 962	500 510	508 295					
1500	175 2181	284 1155	325 685	343 460	359 242				
2000 m/s	*	*	9 1000	43 760	74 526	103 299			

**KEY:** Entries are: h(Km) / Altitude of LEO (Km)  
 h = lower tether length

X = LEO altitude < 200 km  
 \* = h negative

**TABLE 7. TRANSFER TO GEO BY TETHER, WITH  $\Delta V$ 's SUPPLIED BY PROPULSION**

T = 3/8 day

Upper Tether Length H = 8989 Km

$\Delta V_P$	$\Delta V_Q$	0	100	200	300	325	340	350	375	400 m/s
0		1376 2920	1304 1879	1224 944						
300		1121 3176	1092 2091	1049 1119	996 246					
600		846 3450	866 2317	863 1305	843 399					
900		551 3745	624 2558	665 1503	681 561	682 341	682 212			
1200		233 4063	365 2817	454 1714	510 732	519 504	524 371	527 283		
1500		* 3096	86 3096	228 1940	327 915	346 678	356 539	362 447	377 223	
2000		* 993	* 843	* 745	* 505	30 273	51 124	64 273	95 505	124 273

**KEY:** Entries are: h(Km) / Altitude of LEO (Km)

X = LEO Altitude < 200 Km

\* = h negative

17 ORIGINAL PAGE IS  
OF POOR QUALITY

**TABLE 8. TRANSFER TO GEO BY TETHER, WITH  $\Delta V$ 's SUPPLIED BY PROPULSION**

$T = 2/5$  day

Upper Tether Length:  $H = 8271$  Km

$\Delta V_P$	$\Delta V_Q$	0	100	200	300	400	425	450	475	490	m/s
0	1458	1391	1314	1230							
	4047	2875	1826	884							
300	1151	1137	1104	1058							
	4353	3129	2036	1057							
600	821	865	881	875	851						
	4684	3400	2259	1240	329						
900	464	573	642	679	692	692					
	5041	3692	2498	1435	488	268					
1200	76	259	387	472	523	532	539				
	5428	4007	2754	1643	657	428	205				
1500	*	*	111	249	343	361	377				
			3028	1866	837	598	366				
2000	*	*	*	*	17	53	85	115	131		
m/s					1163	907	658	418	277		

**KEY:** Entries are  $h$  (km)/Altitude of LEO  
 $h \equiv$  lower tether length

$X =$  LEO altitude  $< 200$  Km  
 $*$  =  $h$  negative

**Upper Tether Length: H = 5913 Km**

\* = h negative

20

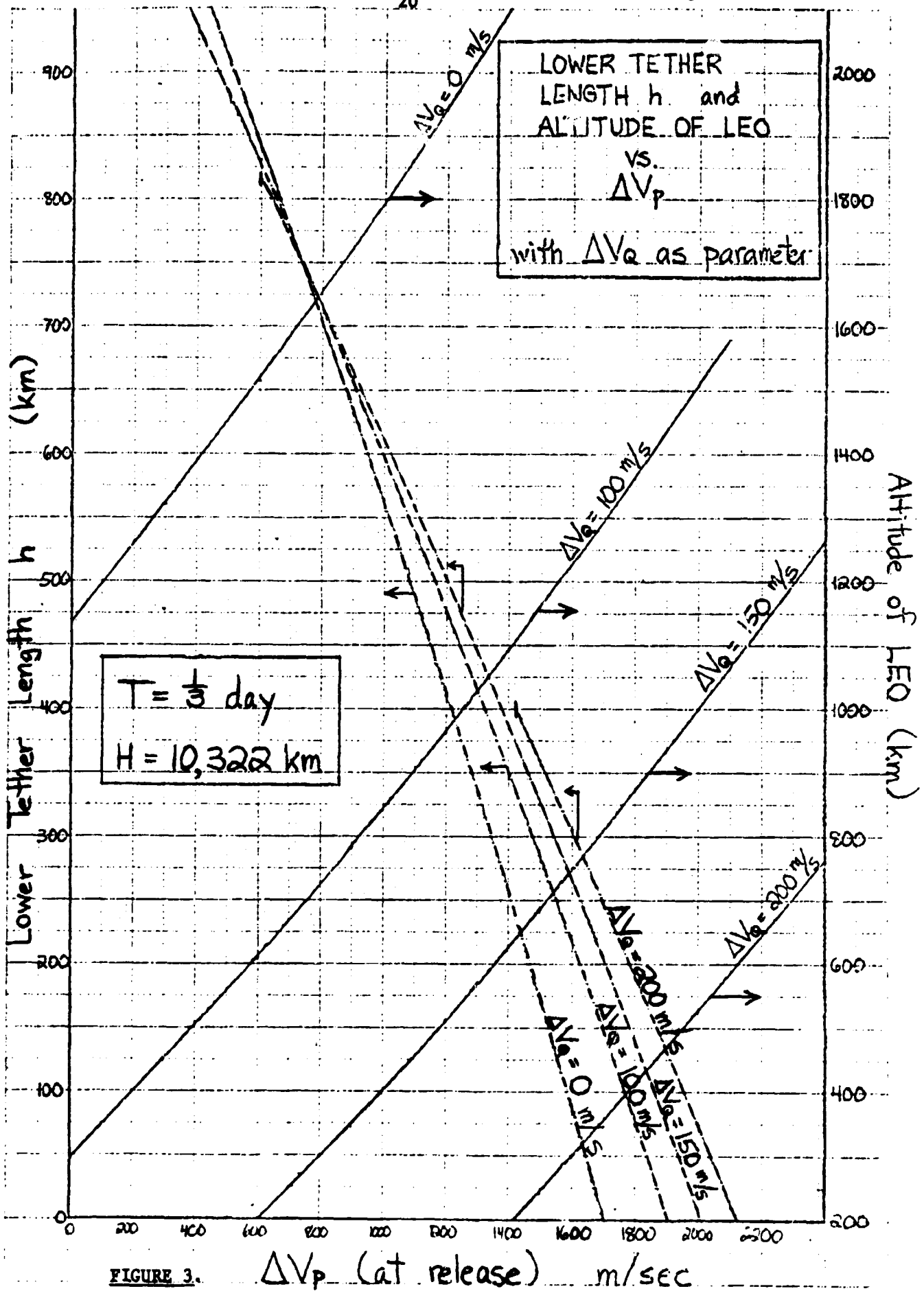


FIGURE 3.



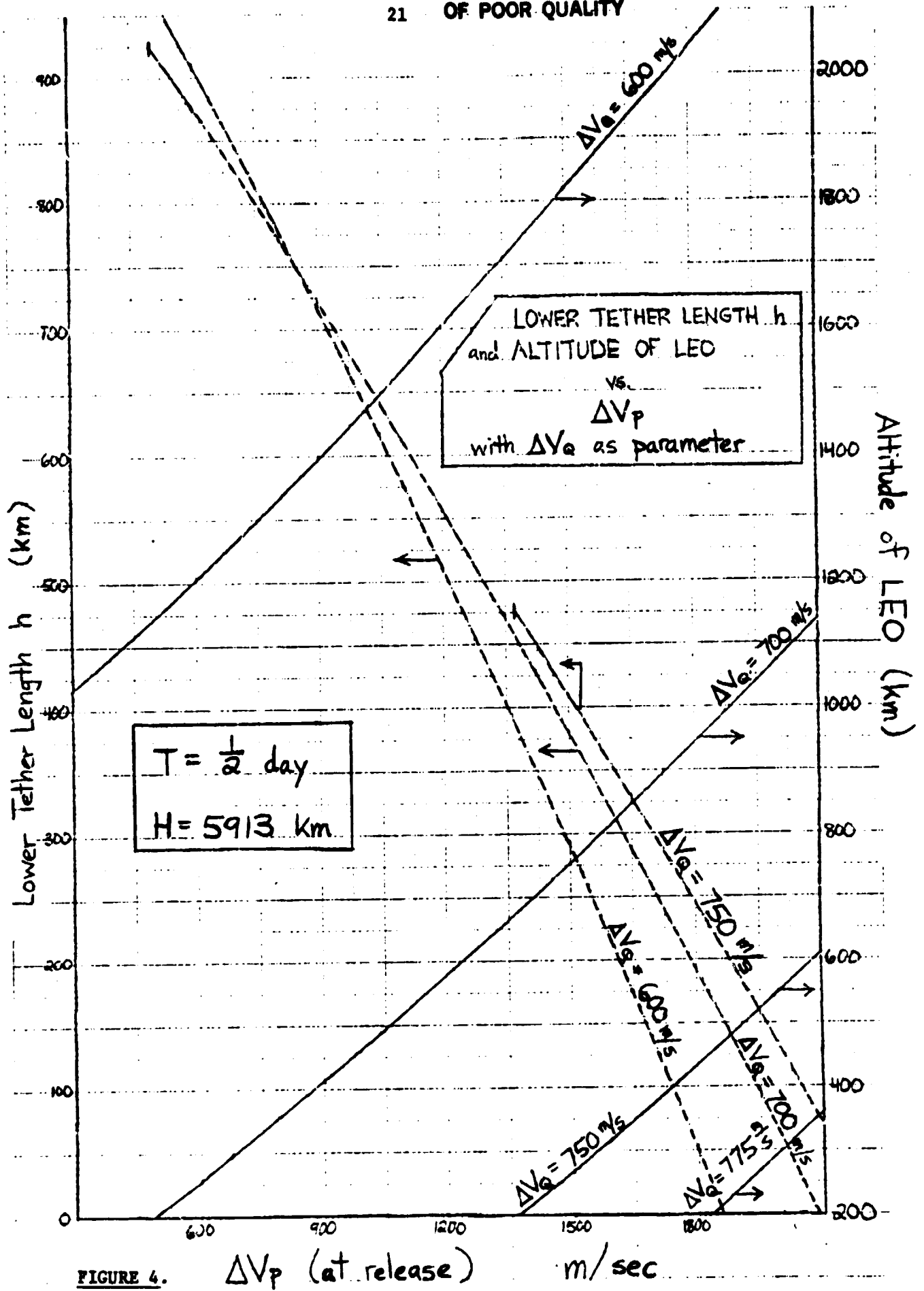


FIGURE 4.

Orbital perturbations of the LEO platform

In the calculations so far we have implicitly assumed very heavy platforms both in LEO and in GEO. If the mass of the LEO platform is dominated by that of the Shuttle orbiter (docked to a light free-flying tether facility, the ratio  $M_{\text{platform}}/M_{\text{payload}}$  may not be very large (3:1 for a 10 Tonne payload). The result may be an excessive lowering of the post-release Shuttle perigee. In this section we consider this effect, while still assuming a massive GEO platform.

The new geometrical arrangement for the lower tether is shown in Fig. 5. The orbital center is at  $R_c$ , given by (Ref. 1).

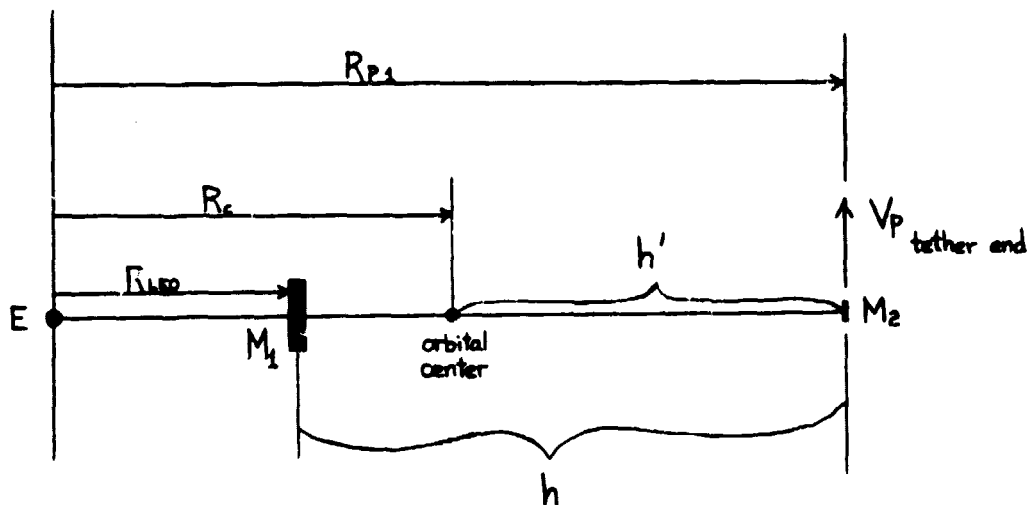


Figure 5. Geometry for a finite lower platform mass.

Ref. 1. Study of Certain Launching Techniques Using Long Orbiting Tethers by Giuseppe Colombo. Final Report on grant NAG-8008, from the SAO to NASA, Feb. 1981.

ORIGINAL PAGE IS  
OF POOR QUALITY

$$R_C = \left( \frac{\sum r_i m_i}{\sum m_i / r_i^2} \right)^{1/3} \quad (17)$$

and is located at a distance  $h' = R_{P_1} - R_C$  from the transfer orbit perigee. Thus,  $h'$  replaces  $h$  and  $R_C$  replaces  $R_{LE}$  in our previous analysis (Eqs. (10, (11) ). The new  $R_{LE}$  must be obtained from the explicit form of Eq. (17); for example, accounting only for two end masses  $M_1, M_2$  (Fig. 5), we have

$$R_C = \frac{R_{LEO} M_1 + R_{P_1} M_2}{M_1 / R_{LEO}^2 + M_2 / R_{P_1}^2} \quad (18)$$

which can be solved for  $R_{LEO}$ .

The perigee of the post-release platform orbit can be calculated from Eq. (6) of Ref. 1, which for our case reads

$$S_2 = -R_{LEO} + 2 / (2/R_{LEO} - R_{LEO}^2 / R_C^3) \quad (19)$$

The effect of this modification is to require a longer lower tether and to make high  $\Delta V_Q$  values unfeasible (negative perigee). As an example, Tables 10 and 11 show a comparison (for 1/3 day period) of two cases, one with a massive LEO platform ( $M_1 = 5000$  Tonne for  $M_2 = 10$  Tonne) and the other with a light LEO platform (the Orbiter,  $M_1 = 80$  Tonne). In the first case, where only a slight perturbation is introduced to the orbit, a tether length  $h = 998$  Km can be used from a 521 Km orbit, which becomes a 521/511 orbit after release. Velocity

TABLE 10. PLATFORM IN LEO

M1 = 5,000,000 kg (platform)

M2 = 10,000 kg (satellite)

P = 1/3 day

H = 10,390 km

$\Delta V_P$	$\Delta V_Q$	0	100	200	300	m/s
0		1229 1217 / 1204	1152 367 / 356			perigee altitude negative ←
100		1168 1278 / 1267	1101 418 / 408			
200		1107 1339 / 1326	1050 469 / 458			
300		1043 1403 / 1391	998 521 / 511			
m/s						

Entries are      h in km  
apogee altitude /  
(km)                      perigee altitude (km)

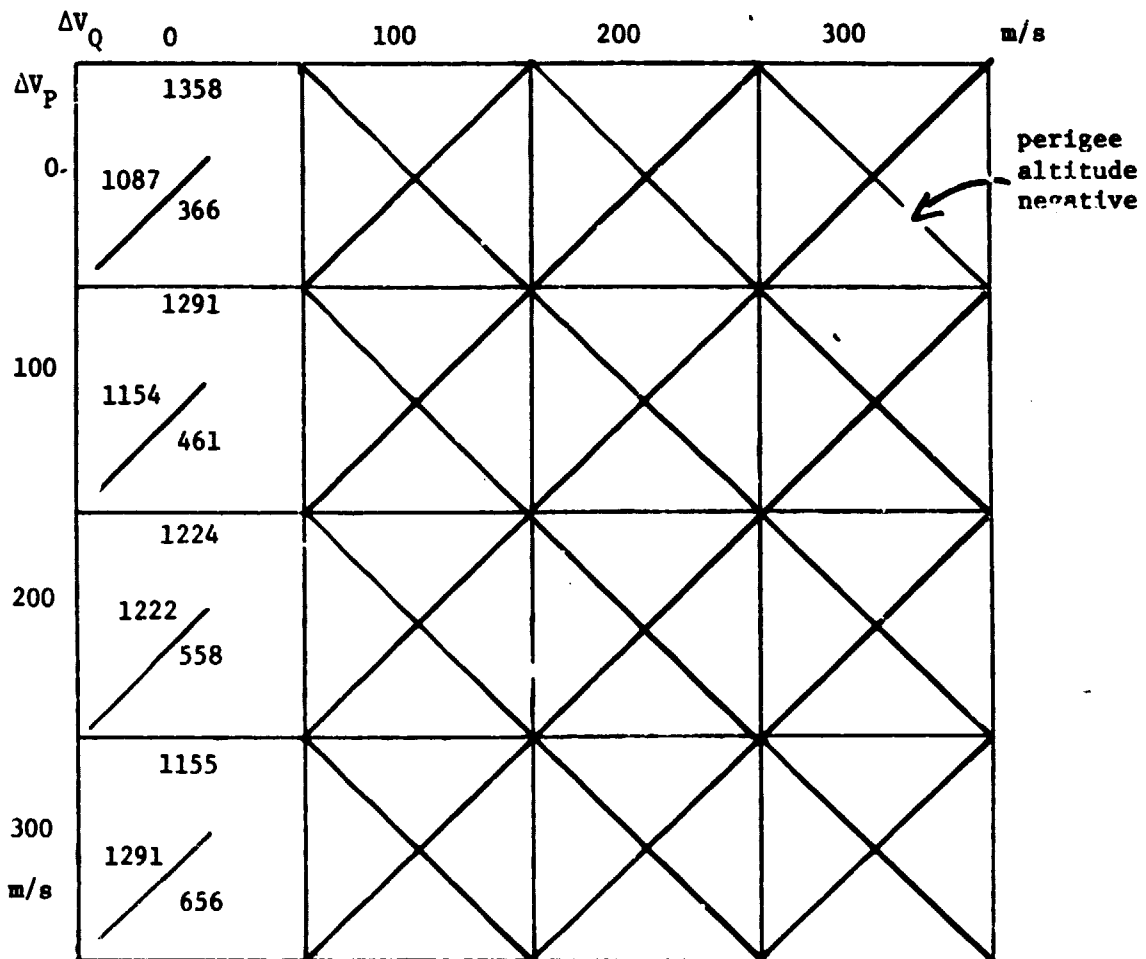
TABLE 11. SHUTTLE IN LEO

M1 = 80,000 kg (shuttle)

M2 = 10,000 kg (satellite)

P = 1/3 day

H = 10,390 km



Entries are

h in km

apogee altitude  
(km)

perigee altitude (km)

increments  $\Delta V_P = 300$  m/sec.  $\Delta V_Q = 100$  m/sec are required. In the case with the light platform, the  $\Delta V_Q = 100$  is not allowable, and so, for  $\Delta V_P = 300$  m/sec, only  $\Delta V_Q = 0$  is possible. The result is a longer tether (1155 Km) and a higher orbit (1291/656).

Work forecast.

In the following period, we anticipate progress on the following points:

- (1) Completion of a trade-off study on the feasible extensions of the Shuttle mission envelope by an on-board tether system.
- (2) Construction of an operational map for the LEO-GEO two-tether system, including the bounds dictated by excessive tether mass and post-release perigee.
- (3) Initial definition of propulsion systems for restoring platform orbits.